

A computational and experimental evaluation of the performance of a centrifugal fan volute

P Dilin^{1*}, T Sakai², M Wilson¹ and A Whitfield¹

¹Department of Mechanical Engineering, University of Bath

²Faculty of Engineering, Mechanical Engineering Division, Science University of Tokyo, Japan

Abstract: A detailed experimental study of the performance of two radial-flow fan volutes has been carried out at the Science University of Tokyo. This included a volute with a full tongue, such that no recirculating flow occurred, and the same volute but with the tongue cut back to allow flow recirculation. Detailed velocity and pressure distributions at a wide range of azimuth angles were obtained experimentally and are presented.

At the University of Bath a computational model, using the $k-\epsilon$ turbulence model, has been used to predict the internal flow of both volutes, with particular attention given to the tongue flow. Predicted flow separation at the volute tongue has been demonstrated experimentally through laser sheet studies at the Science University of Tokyo.

The performance of the volutes is discussed and the computational fluid dynamics (CFD) analysis is used to recommend design improvements for the volute.

Keywords: volutes, fans, internal flow, flow visualization, CFD

NOTATION

B_s	width of the volute cross-section
B_3	width of the diffuser passage at the volute inlet
H_s	height of the volute cross-section
k	turbulent kinetic energy
Q	volume flowrate (m^3/s)
r_3	radius to the diffuser exit or volute inlet
α_3	flow angle at the diffuser exit or volute inlet
ϵ	dissipation rate
θ_s	azimuth angle

1 INTRODUCTION

A spiral-shaped volute is used in many applications of fans and compressors to collect the rotating gas flow, which discharges from the diffuser downstream of the impeller, and to deliver it into a single discharge duct. The performance and design of collecting volutes has not received the detailed study given to the other components of fans and compressors. This can be attributed to the view that the volute is a simple collecting device, all the necessary diffusion having been achieved in the vaned or vaneless diffuser upstream of the volute. In many applications,

however, the overall size of the compressor is very important and the diameter of the diffuser is often less than optimum. In fan applications the diffuser is often dispensed with and the impeller discharges directly into the collecting volute. The volute is usually designed through the application of a one-dimensional analysis assuming a free vortex flow from the volute inlet to the centre of the volute passage [1]. This leads to the flow area, and the radius to its centroid, at any azimuth angle. A design objective is to achieve a uniform pressure distribution at the volute inlet. This is usually attained at the design flowrate only; at off-design conditions the volute is either too small or too large and a pressure distortion develops circumferentially around the volute passage. At low flowrates the pressure increases with the azimuth angle, while at high flowrates the pressure decreases. The static pressure distortions are transmitted to the diffuser exit and to the impeller discharge, and have also been observed through to the impeller inducer [2]. These circumferential pressure distortions reduce the stage performance and have a direct impact on diffuser and impeller flow stability. Qi *et al.* [3] described a volute design technique which allowed a controlled distribution of the volute inlet flow angle, leading to the development of an optimum volute profile.

Detailed published information on the performance of volutes is very limited. Brown and Bradshaw [4] studied a series of symmetrical volute designs with a mixed-flow impeller but found that changes in volute geometry and surface conditions resulted in negligible differences in performance. Stiefel [5] studied the optimization of a radially

The MS was received on 23 February 1998 and was accepted for publication on 3 July 1998.

**Present address: Department of Mechanical Engineering, Huainan Mining Institute, Huainan, Anhui Province, People's Republic of China.*

bladed impeller, vaneless diffuser and an overhung volute. He found that with a vaneless diffuser the optimum volute operation was achieved when the volute was 10–15 per cent smaller than that which would be designed through the frictionless flow assumption. By reducing the size of the volute by 30 per cent Stiefel transformed an unstable performance characteristic to a stable one up to a pressure ratio of 6.3. Stiefel [5] and Whitfield and Roberts [6] showed that the peak efficiency of the compressor stage was close to, but not coincident with, the flow condition, which gave a minimum volute inlet pressure variation with azimuth angle.

The measurement of the complex three-dimensional flow in the volute is difficult, not only due to the complex nature of the flow but also due to the small passages usually involved. Mishina and Gyobu [7] carried out pressure traverses of two volute designs at azimuth angles of 90, 235 and 360°. Axial velocity along the volute passage was shown to decrease with increasing radius from the machine centre-line. Flow in the plane of the section rotated around the centre and appeared to conform well to a solid body rotation; the rotational velocity also diffused around the volute.

In recent years there has been renewed interest in the design and performance of volutes for turbine, compressor and fan applications [3, 8, 9]. For the study presented here a symmetrical volute design with a rectangular cross-sectional area was adopted so that detailed internal flow measurements could be taken. The objective of the investigation was to study the effect of the tongue on the detailed internal flow structure and to provide validation data for the development of computational fluid dynamics (CFD) analysis codes.

2 VOLUTE DESIGN AND TEST FACILITY

For the experimental investigation a symmetrical volute,

Table 1 Geometry of volutes A and C

θ_s (deg)	H_s (mm)	B_s (mm)	Area (mm ²)
35	36.38	29.11	1059
60	48.29	38.63	1865
90	59.89	47.91	2870
120	69.89	55.91	3907
150	78.85	63.08	4974
180	87.09	69.67	6067
210	94.76	75.81	7184
240	102.00	81.6	8323
270	108.88	87.1	9484
300	115.46	92.36	10664
330	121.78	97.42	11863
360	127.87	102.30	13081

made of acrylic resin, was designed at the Science University of Tokyo. The rectangular cross-sectional area had a width–height ratio, B_s/H_s , of 0.8, and the height of the volute passage varied with azimuth angle as

$$H_s \ln \left(1 + \frac{H_s}{r_3} \right) = \frac{\theta_s B_3 \tan \alpha_3}{B_s/H_s} \quad (1)$$

(see reference [1]). The width of the diffuser passage at the volute inlet, B_3 , was 17.6 mm and the corresponding radius, r_3 , was 185 mm. The volute was then designed for an inlet flow angle, α_3 , of 26°. The volute geometry is given in Table 1.

The air was supplied to the volute from a radial flow impeller (diameter of 270 mm) through a vaneless diffuser with a radius ratio of 1.37. The detailed internal flow structure was measured with a five-hole yaw probe constructed from 0.7 mm diameter stainless steel tubing. Access for

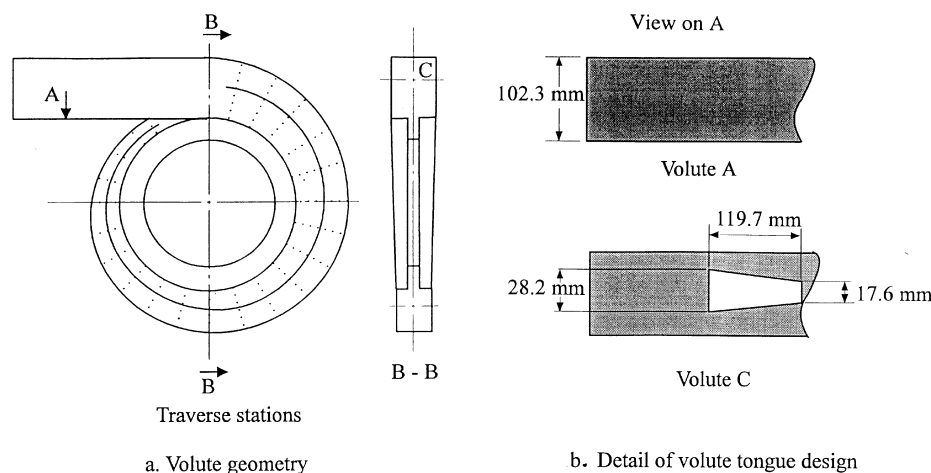


Fig. 1 Volute geometry and flow measurement stations

the probe was provided through the shroud side wall of the volute (Fig. 1a). Traverse measurements were made at the azimuth angle and radial locations shown, and at a range of positions from the hub to the shroud wall surface.

Two volute designs were investigated. For volute A the tongue design was such that it did not allow any recirculation of the air flow. For volute C the tongue design was modified as shown in Fig. 1b, to allow flow recirculation around the volute.

3 COMPUTATIONAL METHOD

Three-dimensional, incompressible, steady flow computations were carried out, at the University of Bath, using the commercially available computational fluid dynamics (CFD) code STAR-CD. This solves discretized forms of the Reynolds-averaged Navier–Stokes equations for turbulent flow using the finite volume method. The unstructured grid solution procedure is based on a variant of the SIMPLE pressure correction technique [10]. The standard form of the high Reynolds number $k-\epsilon$ turbulence model was employed for these calculations, with near-wall conditions supplied by the ‘wall function’ conditions of Launder and Spalding [11].

The grid was generated from the known analytical descriptions of the volute geometry and contained 53 066 fluid cells in total. The vaneless diffuser was discretized by 14×14 grid points on each of the 139 cross-sections. The volute and exit duct were discretized by 14×14 grid points in 167 cross-sections. Cross-sections were concentrated near the tongue region to obtain a more detailed flow description. A three-dimensional view of the discretized flow domain of the volute is shown in Fig. 2.

The inflow boundary conditions were based on known mass flowrates and the flow direction. Uniform velocity

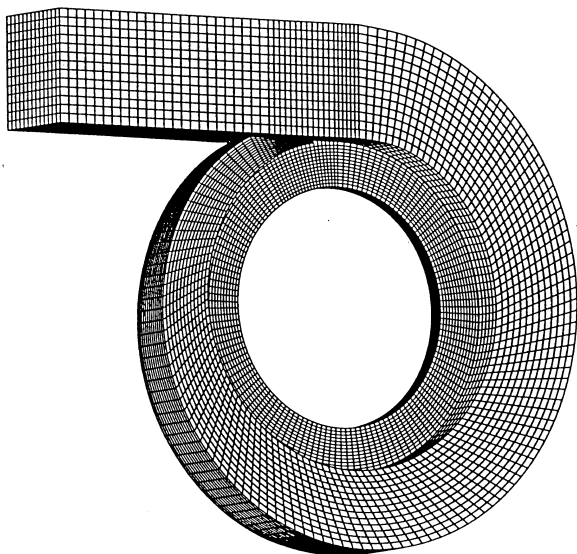


Fig. 2 Three-dimensional view of the discretized flow domain of the volute

profiles were prescribed at the diffuser inlet, according to different flowrates, by specifying radial and tangential velocity components separately. The inlet turbulence level was specified as 10 per cent of the inlet velocity magnitude, but parametric tests suggested that the computed results were not sensitive to this setting. At the outlet, a uniform reference static pressure was imposed.

The iterative solution was deemed to be converged when the normalized absolute error over the mesh had reduced to 1×10^{-5} for each variable, and it was confirmed that solutions were unchanged after further iterations reduced these errors to 1×10^{-6} . The computation time for each case was typically 12 h on a Silicon Graphics R4600PC workstation with a 64 Mb memory.

The sensitivity of solutions to the grid distribution was tested by repeating selected calculations on a finer computational grid which contained 126 600 fluid cells. No significant deviations were observed from the results reported here for the coarser mesh. Hybrid upwind differencing was used for the convective terms in the discretized equations: although available within STAR-CD, blended higher-order schemes have not yet been tested for the three-dimensional flow in the volute. Similarly, the influence of near-wall modelling has not yet been studied, in view of the larger grid and increased computation time associated with a ‘two-layer model’ alternative to the wall function method. The results presented here will provide information for the assessment of more sophisticated computational modelling in the future.

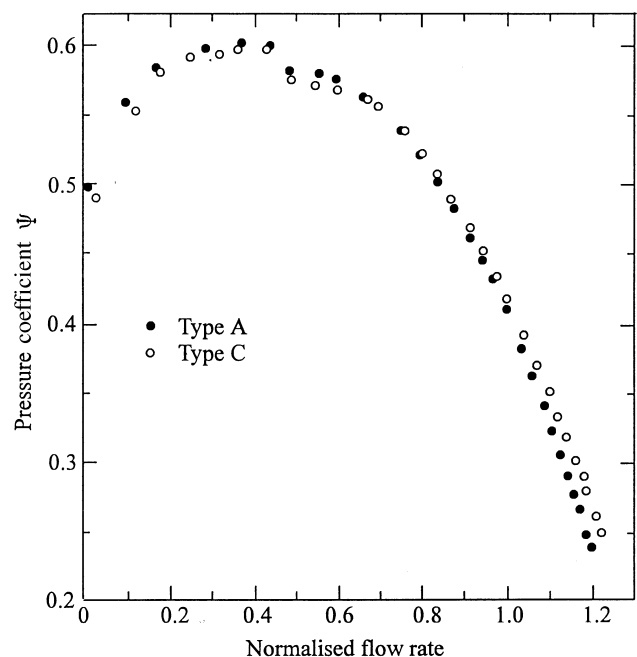


Fig. 3 Fan performance characteristics

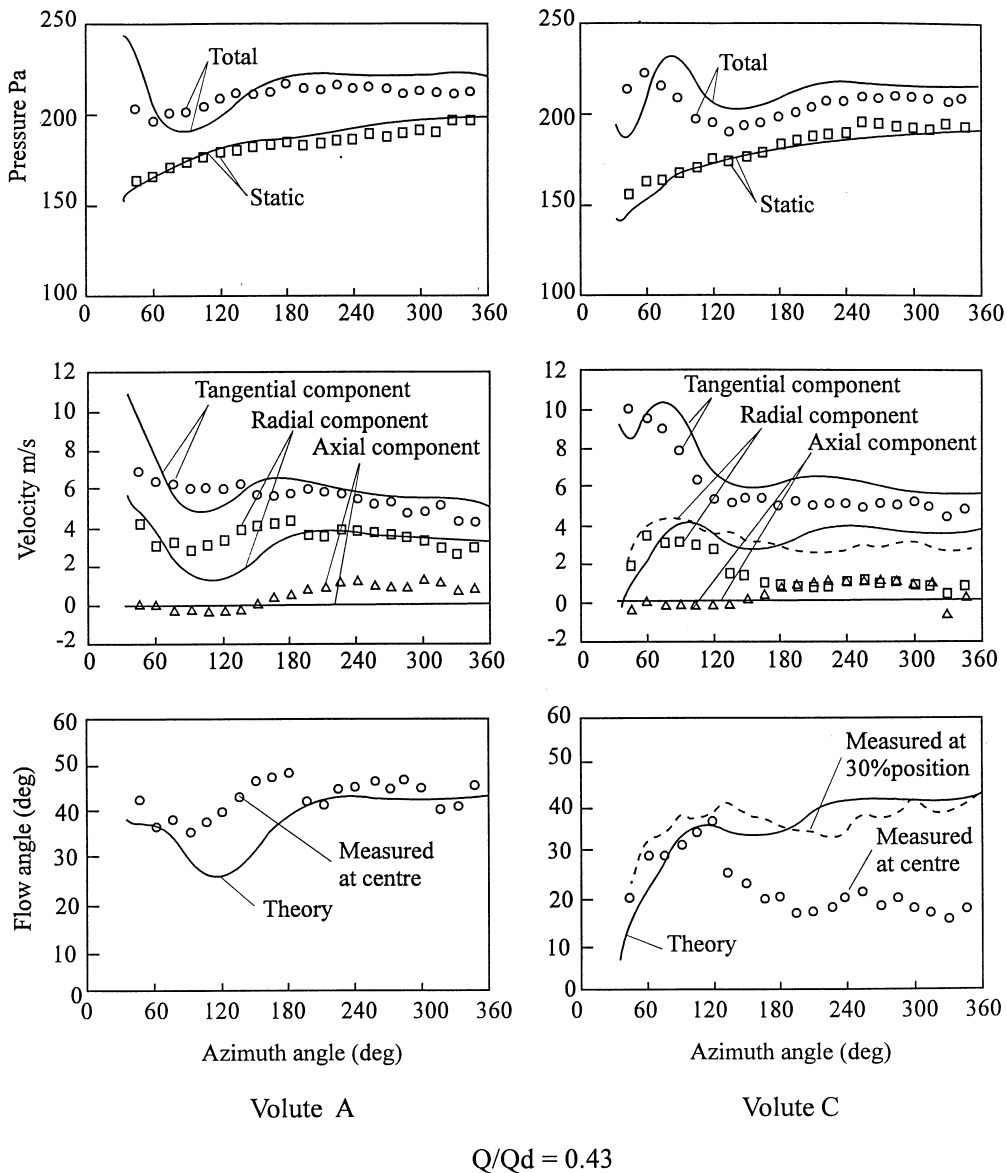


Fig. 4a Variation of the calculated and measured pressures, velocities and flow angles with azimuth angle

4 PRESENTATION AND DISCUSSION OF RESULTS

The basic performance of the fan with volutes A and C is shown in Fig. 3. At high flowrates volute C, with the tongue cut back, led to an improved pressure coefficient. At low flowrates, however, volute A (which did not allow any flow recirculation in the volute) provided a better performance. With both volutes a discontinuity in the performance characteristic was shown at a normalized flowrate of approximately 0.5.

The performance of both volutes, in the form of variation with azimuth angle of measured pressure and flow angle, and derived velocity, is compared with predicted results in Fig. 4. The experimental results were taken at the passage centre (position C in Fig. 1a) and are shown by the plotted

points for three flowrates (Figs 4a, b and c). The theoretical results, shown by the full lines, provide broad agreement with the measurements. The main discrepancy lies with the measured flow angle at the normalized flowrate of 0.43 for volute C (Fig. 4a). Here the measured flow angle shows an uncharacteristic reduction at azimuth angles in excess of 120°; this was not predicted. The predicted flow angle variation with azimuth angle compares well with the measured results when the experimental data are taken at the 30 per cent position rather than at the volute centre, i.e. the 50 per cent position. This indicates that at this low flowrate the air discharging from the vaneless diffuser is directed away from the centre of the passage and towards the hub. The internal flow pattern for volutes A and C are shown in Fig. 5 for the 0.43 flowrate and at azimuth angles of 90° and 345°. For volute A two contrarotating vortices

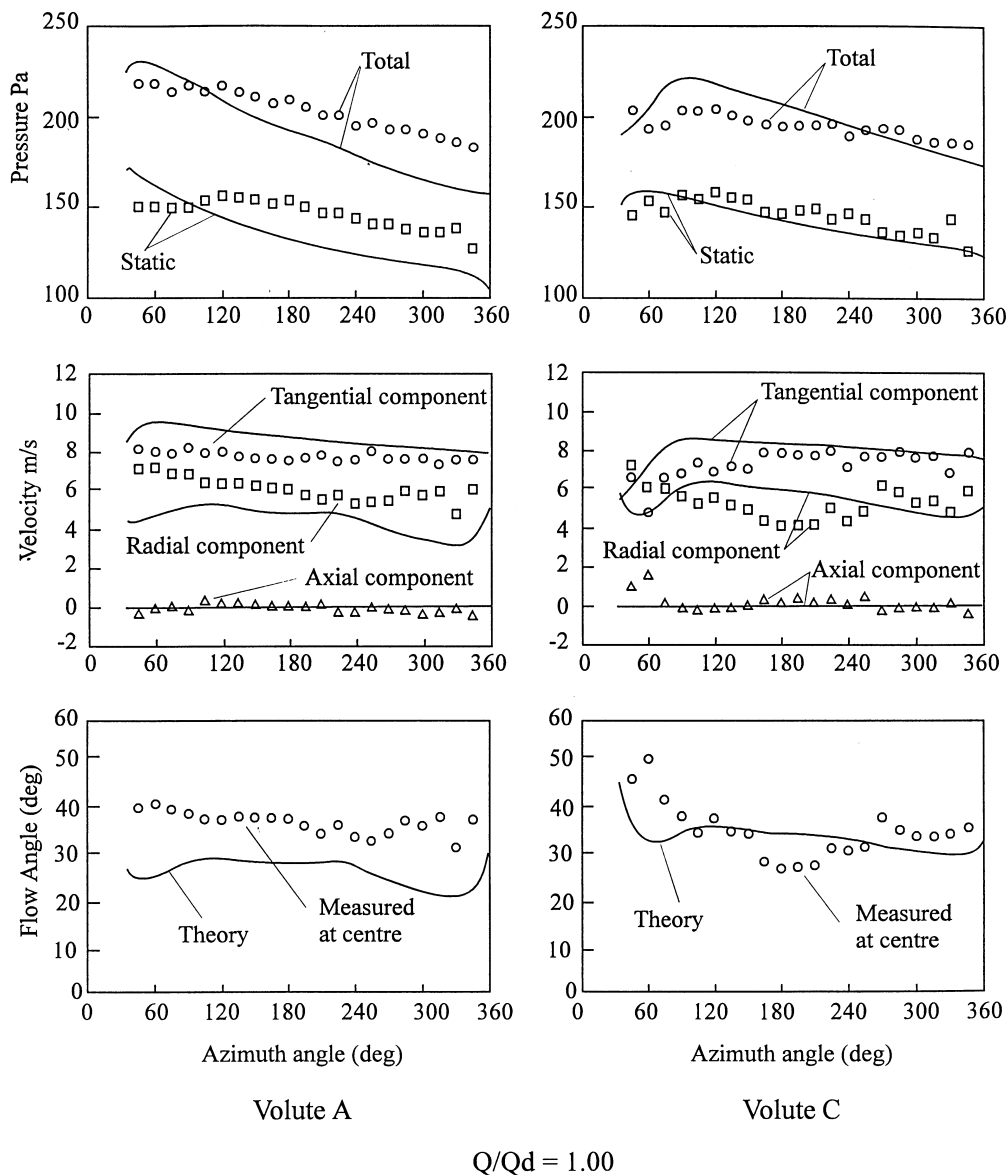


Fig. 4b Variation of the calculated and measured pressures, velocities and flow angles with azimuth angle

are clearly shown, while for volute C a single vortex dominates the cross-section. For volute C the flow at the centre of the cross-section is low at the large azimuth angle, 345° , and provides better correlation with the theoretical results at the 30 per cent traverse station. In other respects the prediction of the flow angle is good, both for magnitude and variation with azimuth angle. For volute A the predicted flow angle tends to be low but the variation with azimuth angle is satisfactory. For volute C the general agreement is good, with the exception described above.

The agreement between measured static and total pressure and the predicted magnitudes is good in terms of both magnitude and variation with azimuth angle. At low flowrates the pressure increases with azimuth angle and at high flowrates the pressure decreases; the rate of decrease of pressure tends to be overpredicted.

The tangential, radial and axial components of velocity were derived from the measured pressures and flow angles. Again good broad agreement is shown between the experimental and predicted results in terms of both magnitude and variation with azimuth angle. At design flowrates the variation of the tangential component of velocity with azimuth angle is represented by the free vortex condition. At off-design flowrates, however, this is not the case, and at high flowrates the tangential component of velocity increases with azimuth angle; i.e. it increases with radius.

The measured and predicted flow angles across the inlet cross-section of the volute at azimuth angles of 90° and 345° are shown in Fig. 6 for three flowrates. The non-symmetrical nature of the angle distribution at low flowrates can be clearly seen. With volute A the distribution is symmetrical except at the low flowrate and at an azimuth

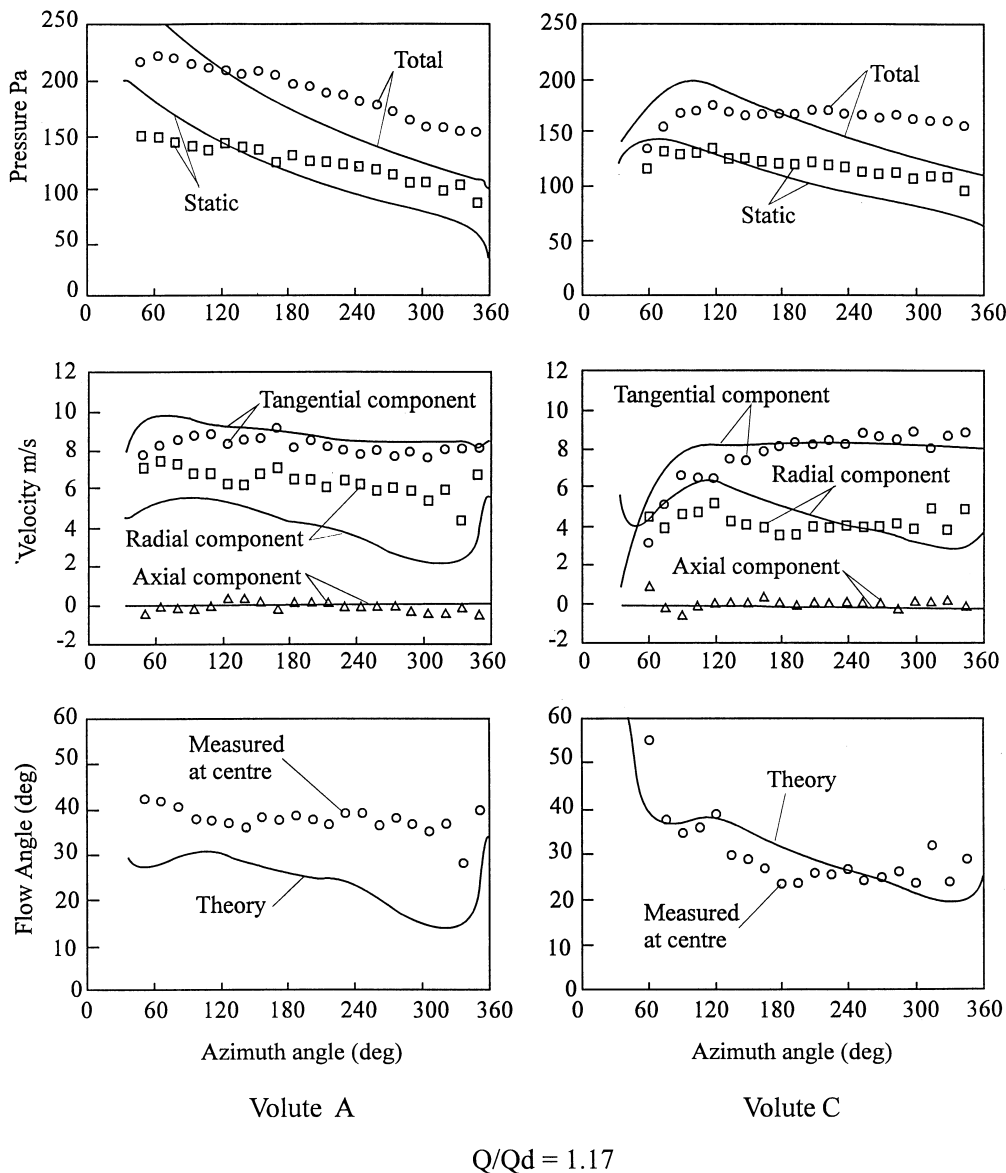


Fig. 4c Variation of the calculated and measured pressures, velocities and flow angles with azimuth angle

angle of 90°, where the flow is pushed towards the shroud; this can be seen in Fig. 5. With volute C the lack of symmetry exists at both azimuth angles and in this case the flow is pushed towards the hub and a single vortex dominates (see also Fig. 5). The predicted results are always symmetrical due to the uniform velocity profile specified at the inlet.

The direct impact of the tongue modifications on the predicted internal flow pattern is illustrated in Fig. 7. Cutting the tongue back (volute C) allows air to recirculate at the low flowrates. As the flowrate is increased, however, recirculation around the volute does not occur and the air is forced over the tongue. The full tongue of volute A, which eliminates most of the recirculating flow at low flowrates, leads to a more distorted flow structure as the flowrate is increased (Fig. 7). This could account for the reduction in

the fan's performance at large flowrates with volute A (see Fig. 3).

Although the experimental results obtained with the yaw probe do not provide sufficient detail to make direct comparisons in the tongue region, they do give evidence to support these predictions. The measured data show that for volute C the flow angle in the region of the tongue is very small (about 10°) at low flowrates and that it increases with increasing flowrate. At the highest flowrate the flow angle is of the order of 55° (Fig. 4c). As a consequence, at low flowrates (Fig. 4a) for azimuth angles less than 60°, the tangential velocity component is much larger than that at high flowrates (Fig. 4c). These results indicate that at low flowrates, because of recirculation, the flow beneath the tongue is almost circumferential, while at high flowrates the flow from the volute towards the exit duct makes a high

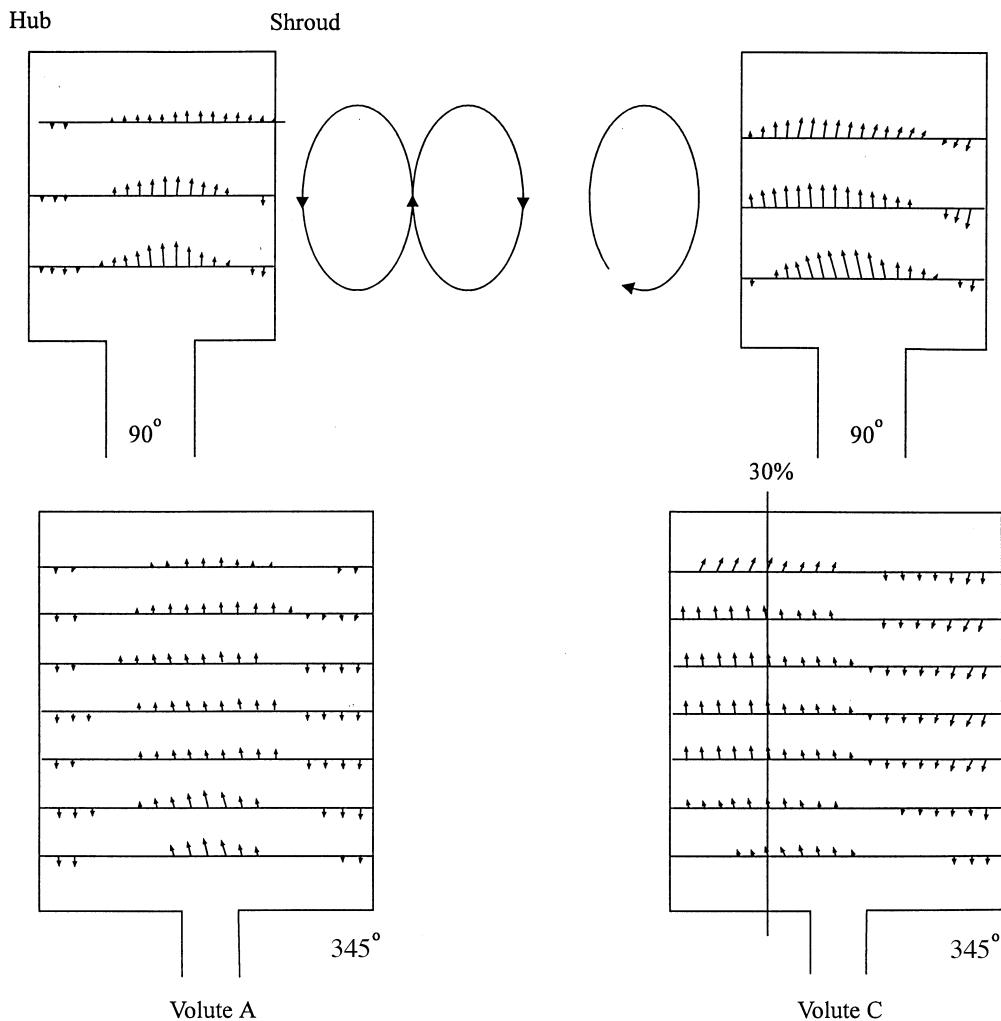


Fig. 5 Volute flow patterns $Q/Q_d = 0.43$

flow angle in the region just after the tongue. Because of the deep tongue there is no experimental data available to illustrate the flow patterns underneath the tongue for volute A.

The comparison of measured flow angle across the inlet cross-section of the volute at azimuth angles of 90° and 345° (Fig. 6) gives further confirmation for the predicted flow patterns. At low flowrates the maximum flow angle inside volute C reduced from 34° at an azimuth angle of 90° to 27° at an azimuth angle of 345° (Fig. 6b). In volute A the maximum flow angle remained almost constant with azimuth angle at low flowrates (Fig. 6a). At the highest flowrate the maximum flow angle in volute A increased by approximately 12° , from 40° at an azimuth angle of 90° to 52° at an azimuth angle of 345° . The flow angle in volute C increased by about 8° . An increasing flow angle indicates that the air in both volutes A and C is directed into the exit duct.

The predicted volute tongue flow (Fig. 7) was further investigated experimentally at the Science University of Tokyo using a laser sheet flow visualization study. The

passage of soap bubbles injected into the volute flow was video-recorded; the results shown in Fig. 8 are a compilation of a series of soap bubbles injected into the air stream at different times. The severe separation of the flow from the tongue of volute A at high flowrates is clearly shown by the flow visualization, and the experimental results (Fig. 8) show excellent qualitative agreement with those predicted (Fig. 7). Cutting back the tongue, volute C, reduced the magnitude of the separated flow region, as predicted.

4.1 Application of the CFD analysis to volute design

As a theoretical assessment the computational procedure was applied to the design of volute C to see if it could be improved; the modified design was not, however, manufactured for experimental study. The basic free vortex design procedure [1] can only give a circumferentially uniform flow at the design flow condition. For the actual three-dimensional flow in a volute the inlet flow angle cannot be maintained constant with azimuth angle. Yao *et al.*

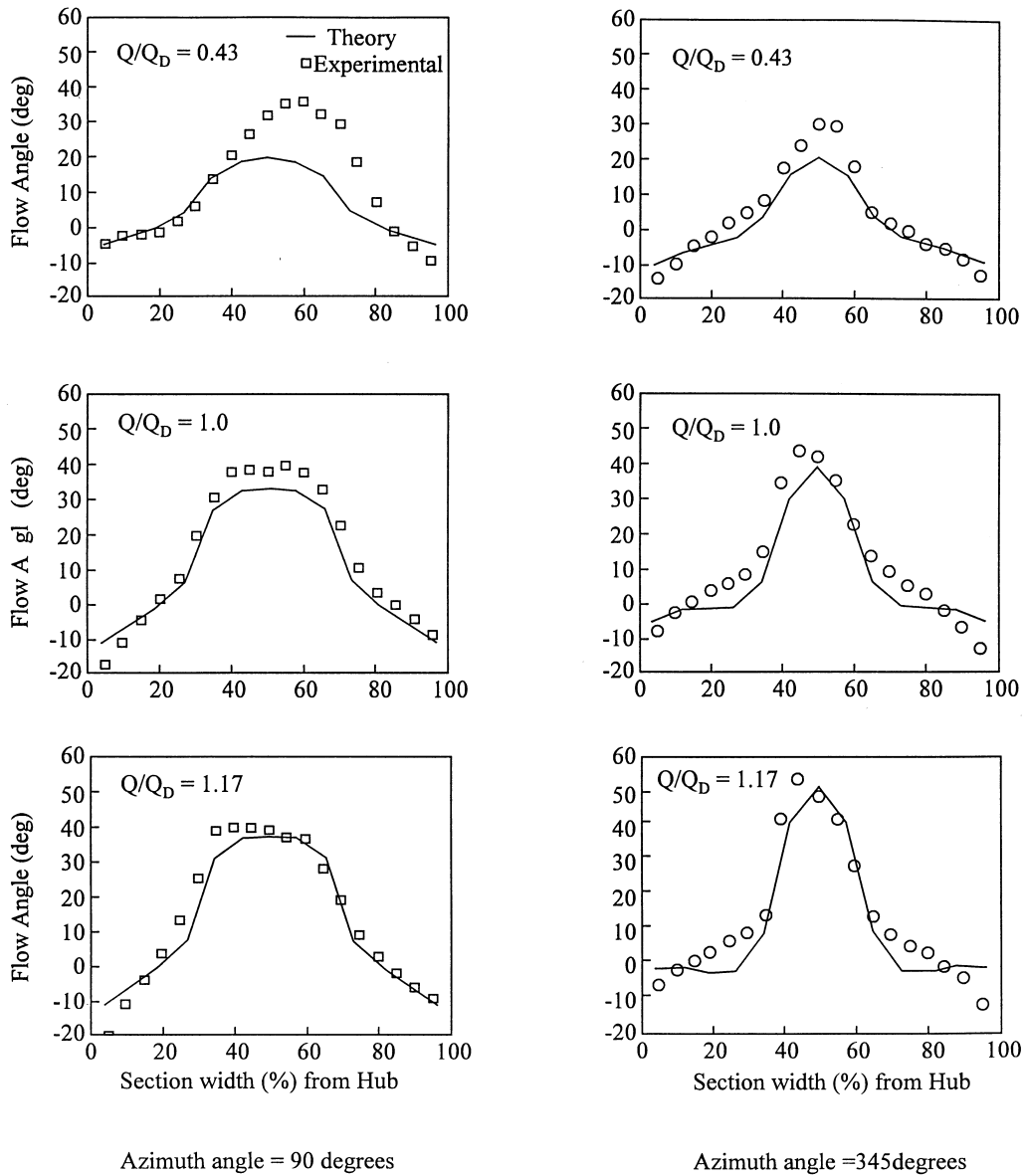


Fig. 6a Measured and calculated flow angles near the volute inlet (volute A)

Table 2 Modified volute geometry

θ_s (deg)	H_s (mm)	B_s (mm)	Area (mm ²)
35	43.19	34.56	1493
60	56.48	45.18	2552
90	68.71	54.97	3777
120	78.56	62.85	4937
150	86.76	69.41	6023
180	93.72	74.98	7027
210	99.66	79.73	7947
240	104.75	83.8	8778
270	108.88	87.1	9484
300	115.46	92.36	10664
330	121.78	97.42	11863
360	127.87	102.30	13081

[12] proposed a design procedure that no longer considered the flow angle, α_3 in equation (1), to be constant. This design procedure, which was further developed by Qi *et al.* [3], allows alternative volute profiles to be developed by varying the volute inlet flow angle α_3 . This procedure was applied, in the computations, through the specification of a non-uniform inlet flow angle, as shown in Fig. 9. The flow angle at the cut-off point was specified as 34° and allowed to decrease linearly to 26° at an azimuth angle of 270° . Equation (1) was then applied to give the modified volute profile shown in Fig. 10 and detailed in Table 2. The modified design provides an enlargement of the flow passage underneath the tongue by about 12 per cent, and the minimum radial clearance between the tongue and the

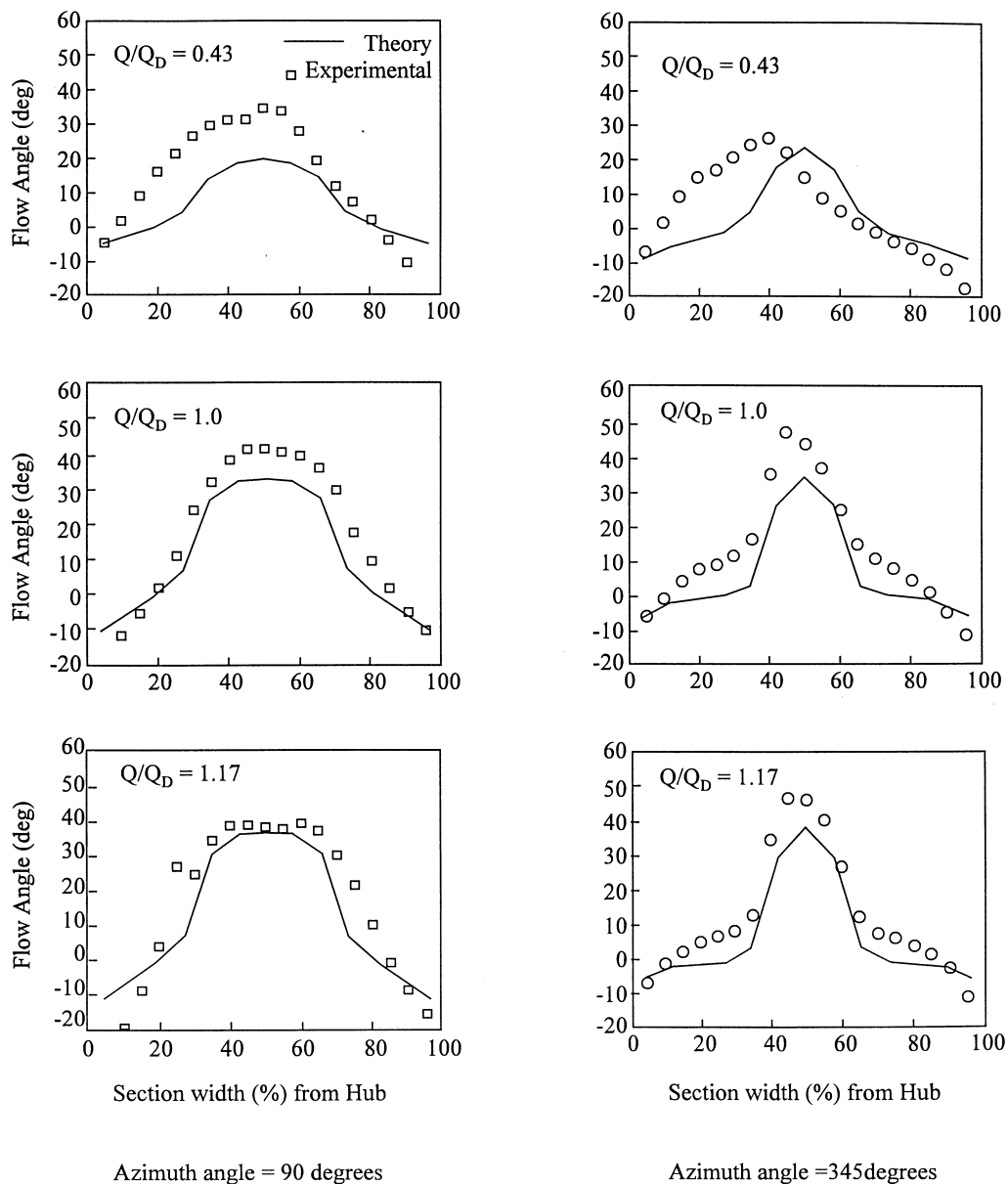


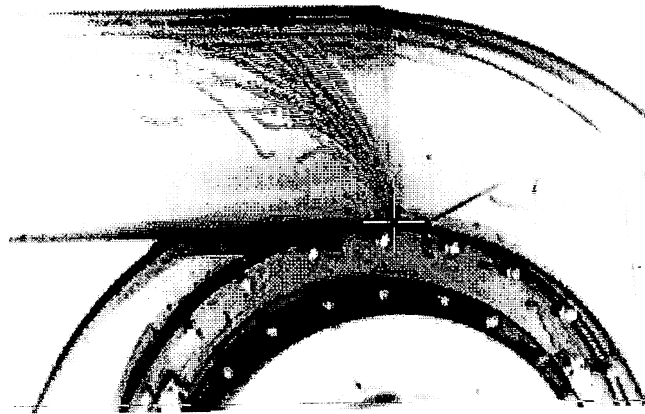
Fig. 6b Measured and calculated flow angles near the volute inlet (volute C)

diffuser outlet is also increased. The original sharp-pointed tongue was also rounded as shown. This modification to the tongue alone had no significant effect on the predicted results. The predicted variations of flow parameters with azimuth angle are shown in Fig. 11 for the modified and original volutes. This shows the effect of the volute design on the predicted flow parameters at the diffuser inlet and discharge (volute inlet). The modified volute design has led to a reduction in the flow distortion at the diffuser inlet and outlet at all flowrates, but particularly at off-design flowrates. The difference between the peak and minimum magnitudes of pressure was reduced by approximately 25 per cent at both low and high flowrates when the modified design was applied. At the design flowrate the original

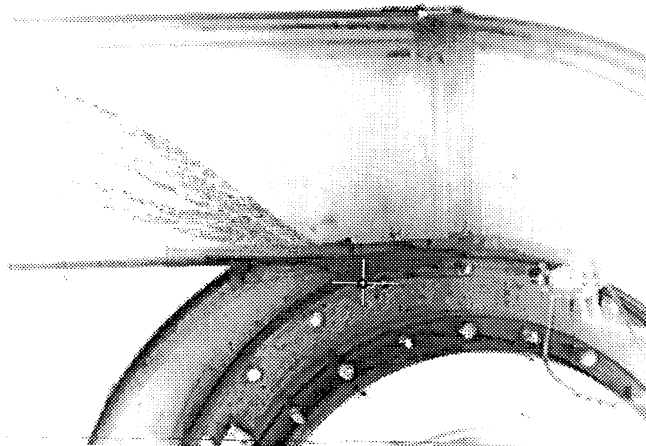
volute design showed a better performance in terms of the variation of pressure and flow angle with azimuth angle. At the design flowrate the assumption of a constant flow angle, α_3 , is clearly better, but at off-design flowrates the modified design shows improved distributions with azimuth angle.

5 CONCLUSIONS

The experimental and computational investigation provided a satisfactory means of assessing the internal flow structure and performance of the symmetrical volute. The CFD code STAR-CD was used to model the flow in the volute, with



$Q/Q_d=1.17$ Volute A



$Q/Q_d=1.17$ Volute C

Fig. 8 Laser sheet flow visualization at the volute tongue

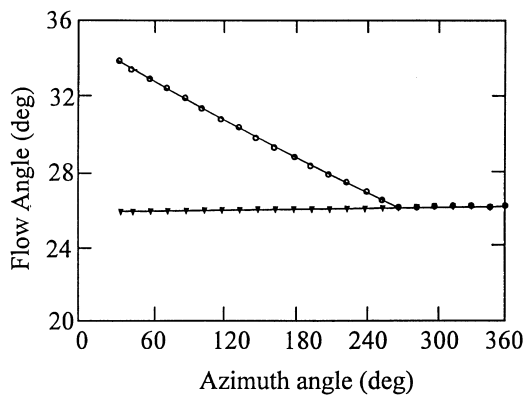


Fig. 9 Specified inlet flow angle for the volute design

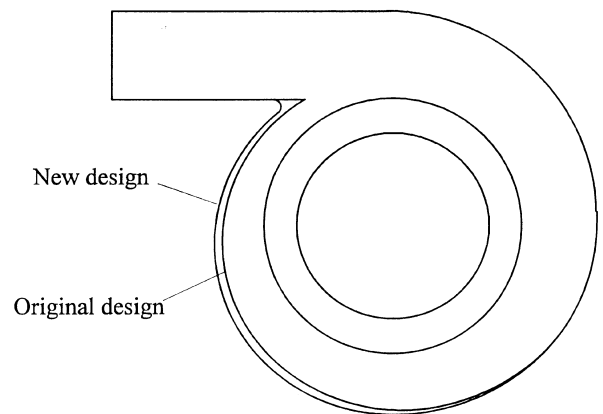


Fig. 10 The geometric rearrangement of the volute

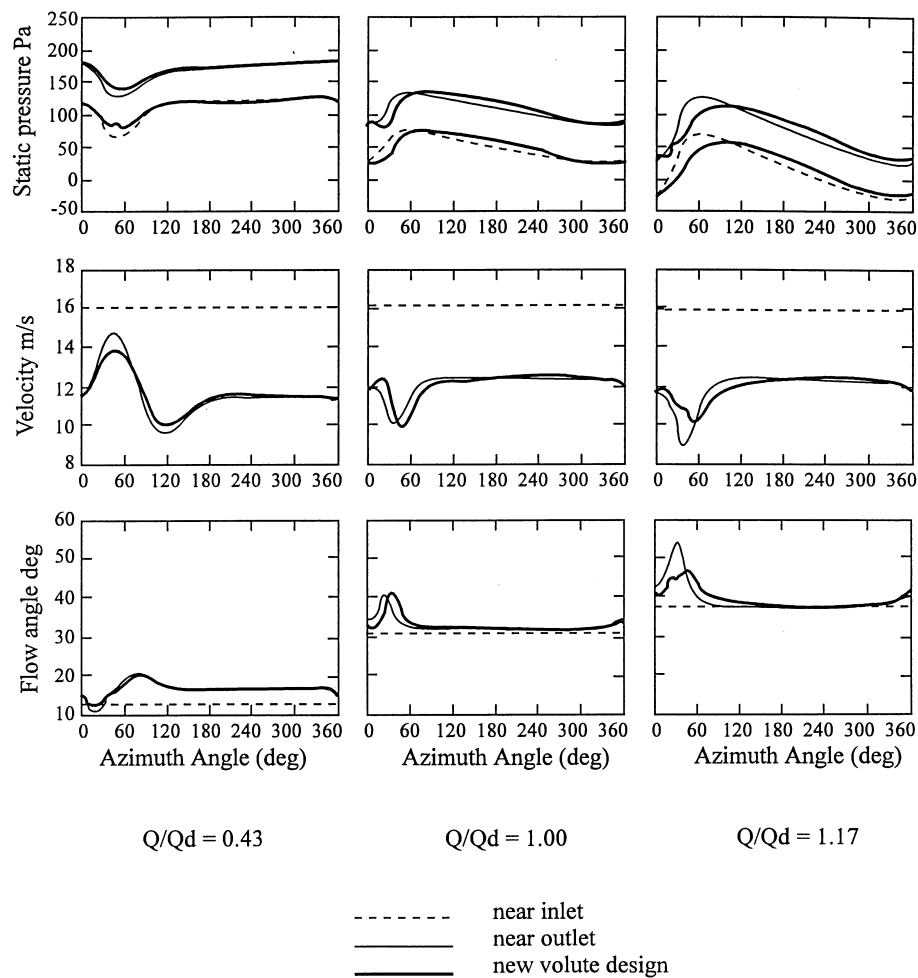


Fig. 11 Effect of the volute design on predicted pressure, velocity and flow angle profiles at the diffuser inlet and outlet

REFERENCES

- 1 Eck, B. *Fans*, 1973 (Pergamon Press, Oxford).
- 2 Fink, D. A., Cumpsty, N. A. and Greitzer, E. Surge dynamics in a free-spool centrifugal compressor system. *Trans. ASME, J. Turbomachinery*, **114**, 1992, 321–332.
- 3 Qi, D. T., Promfret, M. J. and Lam, K. A new approach to the design of fan volute profiles. *Proc. Instn Mech. Engrs, Part C, Journal of Mechanical Engineering Science*, 1996, **210**(C3), 287–294.
- 4 Brown, W. B. and Bradshaw, G. R. Design and performance of a family of diffusing scrolls with mixed flow impeller and vaneless diffuser. NACA Report 936, 1974.
- 5 Stiefel, W. Experience in development of radial compressors. VKI Lecture Series 50, 1972.
- 6 Whitfield, A. and Roberts, D. V. Alternative vaneless diffusers and collecting volutes for turbocharger compressors. In ASME 28th International Gas Turbine Conference, Phoenix, Arizona, 1983, paper 83-GT-32.
- 7 Mishina, H. and Gyobu, I. Performance investigations of large capacity centrifugal compressors. In ASME 23rd International Gas Turbine Conference, London, 1978, paper 78-GT-3.
- 8 Ayder, E., Van den Braembussche, R. and Brazz, J. J. Experimental and theoretical analysis of the flow in a centrifugal compressor volute. *Trans. ASME, J. Turbomachinery*, 1993, **115**, 582–589.
- 9 Chen, H. Design methods of volute casings for turbocharger applications. *Proc. Instn Mech. Engrs, Part A, Journal of Power and Energy*, 1996, **210**(A2), 149–156.
- 10 Patankar, S. V. *Numerical Heat Transfer and Fluid Flow*, 1980 (Hemisphere).
- 11 Launder, B. E. and Spalding, D. B. The numerical computation of turbulent flow. *Comput. Meth. Appl. Mechanics*, 1974, **3**, 269.
- 12 Yao, C. F., *et al.* Study on the scroll of the fan with high efficiency and low noise (in Chinese). *Fluid Engng*, 1991, **19**(7), 2–6.